Mikrochim. Acta 132, 67–77 (1999)

Mikrochimica Acta

Voltammetry of Organic Microparticles

Šebojka Komorsky-Lovrić[1], **Valentin Mirčeski**[2], and **Fritz Scholz**[3]

[1] Center for Marine Research Zagreb, "Ruder Bošković" Institute, POB 1016, HR-10001 Zagreb Croatia
[2] Institute of Chemistry, Faculty of Natural Sciences and Mathematics, "Cyril and Methodius" University, POB 162, MAK-91001 Skopje Macedonia
[3] E.-M.-Arndt-Universität Greifswald, Institut für Chemie, Soldtmannstraße 23, 17489 Greifswald Germany

Abstract. Solid microparticles of several different insoluble organic compounds were mechanically immobilized on the surface of graphite electrodes and immersed into a liquid electrolyte in order to study their electrochemical reactions. Cyclic staircase voltammetry and square-wave voltammetry were used. Quinhydrone was found to be a stable intermediate in the reversible redox reaction of solid quinone and hydroquinone on the electrode surface. The reaction occurs on the surface of the solid particle which is in contact with water. Indigo can be reduced to leucoindigo and oxidized to dehydroindigo in two separate reversible redox reactions. In strongly basic medium indigo dissolves in water upon electroreduction. A hydroacridine radical was detected as a stable intermediate in the electrochemically irreversible redox reaction of acridine and dihydroacridine. Famotidine can be electrooxidized and the product of this reaction can be electroreduced in two separate chemically irreversible reactions. Probucol is oxidized to a semiquinone radical which can be re-reduced in an electrochemically irreversible redox reaction. Propylthiouracil can be also oxidized to an unknown product which can be re-reduced in a chemically reversible, but slow solid state surface redox reaction. Reductions of solid thionicotinoylanilide and nicotinoylanilide are totally irreversible.

Key words: solid state voltammetry; quinhydrone; quinone; hydroquinone; indigo; leucoindigo; acridine; famotidine; probucol; propylthiouracil; thionicotinoylanilide; nicotinoylanilide.

Electrochemical methods can be used for qualitative and quantitative analysis of solids [1]. Electroanalysis can provide information on the composition of powder mixtures [2], minerals [3] and alloys [4], as well as on the structure of some solid compounds [5]. Besides, it was applied for the detection of electroactive impurities in inert solid samples [6], such as manganese ions in carbonate sediments [7], and for the identification of solid contaminants, such as traces of cocaine on paper [8]. For electroanalytical purposes the most convenient technique is voltammetry of immobilized microparticles [9,10]. This method is based on the mechanical transfer of insoluble solid microparticles on the surface of a carbon rod which is used as a working electrode in standard voltammetric experiments. Redox reactions which are measured by this procedure can be either destructive, i.e. leading to a dissolution of the particle, or not, depending on the solubility of the reaction products. Reductions of metal ions in oxides, oxyhydroxides, sulfides and some minerals to the metallic state [11–16], as well as the oxidation of metal deposits [17–19] are examples of the first group of reactions. Intercalation, or insertion and the surface redox reactions are nondestructive processes. Insertion compounds are both ionic and electronic conductors. The change of charge on the metal ions in these compounds, which occurs in their electrochemical reactions, is accompanied by the exchange of charge compensating ions with the liquid electrolyte and by their diffusion through the particle body together with the propagation of electrons. So, the transfer of an electron across the electrode|particle interface and the transfer of an ion at the particle|solution interface occur simultaneously. This type of reactions was observed with some metal oxides and

complexes [20–22], metal hexacyanometallates [23–28] and several organometallic and organic compounds [29–37]. The surface reactions are localised on the particle | electrolyte interface. They are characteristic for redox reactions which are coupled with the exchange of protons between some insoluble organic compounds and the dissolved acids or bases [38–41]. Localization is a consequence of the fact that proton donors cannot penetrate the surface of the organic particle [41, 42]. In all three types of reactions the depolarization starts at the three phases boundary, at which the electrode, the particle and the electrolyte are in contact [43–45]. From there the redox reaction expands over the surface and into the body of the particle by the electronic and ionic conductivity of the solid. If only the conduction of ions is hindered, the reaction will be localized at the particle | solution interface, while if only the electronic conductivity is poor, the reaction may occur in the electrode | particle interface. Electronic conductivity can be metallic or faradaic. Faradaic conductivity was observed with electroactive solids which do not conduct electrons when they are dry. If these insulators are brought into contact with an electrolyte, either liquid or solid, the electrons are propagated by a series of faradaic reactions which are accompanied by the exchange of ions or protons with the electrolyte. This conductivity is a consequence of the gradient of the electrochemical potential in the solid particle. For better understanding of these phenomena it is necessary to gather as many experimental data as possible. In this communication the results of voltammetric experiments with solid microparticles of quinhydrone, indigo, acridine, famotidine, probucol, propylthiouracil and thionicotinoylanilide are reported. The first three organic compounds are chosen as model substances because their redox reactions in solvents are well known and hence the voltammetric responses of their microparticles can be interpreted with a certain accuracy. The last four compounds are used as drugs, but their redox reactions are unknown. Voltammetric responses of these substances are explained by the comparison with the model compounds. The goal is to establish a basis for the development of electroanalytical methods for a direct identification of powders.

Quinhydrone ($Q*H_2Q$) is a 1:1 molecular complex between quinone (Q) and hydroquinone (H_2Q) [46, 47]. In crystals the molecules are connected by hydrogen bonds between the hydroxyl group of hydroquinone and the carbonyl group of quinone. Thus they form infinite molecular chains. These chains are packed in sheets by charge transfer interactions and van der Waals forces [47]. Quinhydrone is practically insoluble in cold water, but soluble in hot water. When dissolved it dissociates in quinone and hydroquinone forming a well known redox couple [48, 49]. In a buffered water solution its polarographic response is a single, reversible, two-electrons wave: $Q + 2e^- + 2H^+ \rightleftharpoons H_2Q$ [49]. Electroactive species are Q and Q^{2-}, but the divalent Q^{2-} is in a protolytic equilibrium with HQ^- and H_2Q [50]. In organic, aprotic solvents quinhydrone is a mixture of two redox couples [48]. Quinone is reduced to a dianion which is protonated by hydroquinone: $Q + 2e^- + H_2Q \rightarrow 2HQ^-$. Oxidation of hydroquinone involves the transfer of two electrons and the protonation of quinone: $H_2Q + Q \rightarrow 2HQ^+ + 2e^-$ [51].

Indigo is a well known dye which is extremely insoluble in water [52]. In a suspension in strongly alkaline aqueous solution it can be reduced by sodium dithionite or iron(II)triethanolamine complex to soluble leucoindigo which may then be oxidized back to the original indigo by oxygen [53]. Indigo dissolved in pyridine can reversibly be electroreduced to leucoindigo on a mercury electrode in presence of pyridinium nitrate as an electron donor [54] (Scheme 1).

The same reversible redox reaction was observed in aqueous electrolytes of various pH when indigo was incorporated in polypyrrole film on a platinum disk electrode [55] and when leucoindigo was immobilised as a thin film on the surface of a platinum electrode [56]. Indigo can be oxidised by ozone to isatin and isatoic anhydride [57]. In acidic and neutral aqueous

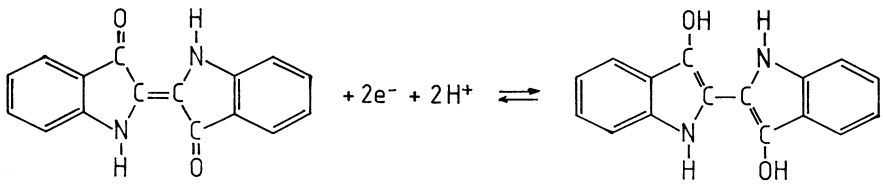

Scheme 1

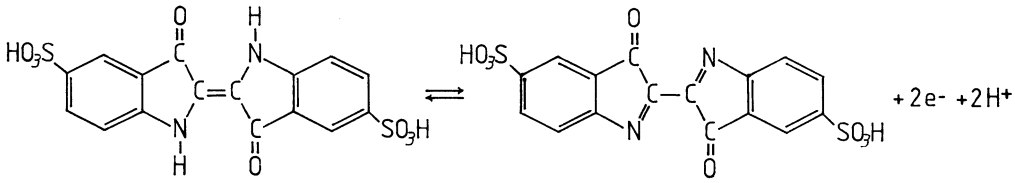

Scheme 2

electrolytes on a platinum electrode indigo carmine which is soluble in water undergoes reversible electrooxidation to dehydroindigo [58] (Scheme 2).

Isatin may appear as a product of electrooxidation at potentials positive to 0.8 V vs SCE in basic media. Solid indigo is a p-type semiconductor with the specific resistance of $10^9\,\Omega$ cm [59]. The electrochemical properties of solid microparticles of indigo were investigated by Bond et al. [40]. The particles were mechanically attached to the graphite electrode surface and immersed in an aqueous electrolyte solution. In cyclic voltammetry two well developed pairs of responses were observed and attributed to reversible reactions of indigo-leucoindigo and indigo-dehydroindigo redox couples. It was proposed that the redox reactions spread over the surface of microparticles by series of electron hoppings between the neighbouring molecules. In the first cycle this process required higher overvoltage than in the subsequent cycles. This was termed a "break in" phase and explained as an activation of the surface. In 0.1 M NaOH solution, a dissolution of leucoindigo was observed.

Acridine is electroreduced in two stages. The product of the first redox reaction is a monohydroacridine radical, and in the second stage dihydroacridine is formed [60–62].

Famotidine (I), probucol (II), propylthiouracil (III), nicotinoylanilide (IV) and thionicotinoylanilide (V) are pharmacologically active compounds which are used for the treatment of gastrointestinal ulcers, as a cholesterol-lowering agent, a thyroid depressant and a potential tuberculostatics, respectively [63]. Famotidine can be oxidized on glassy carbon electrode at 0.85 V [64] and reduced on a mercury electrode at −1.3 V [65]. Generally, thiones can be reduced on a platinum electrode at potentials between −0.5 V and −1.5 V [66]. Electrochemical properties of other compounds are not known.

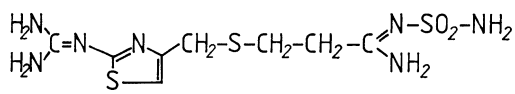

(I) (famotidine)

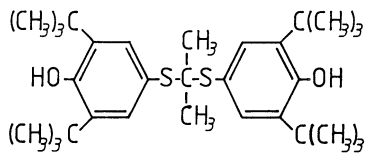

(II) (probucol)

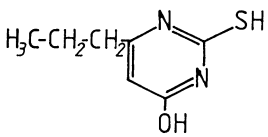

(III) (6-propyl-2-thiouracil)

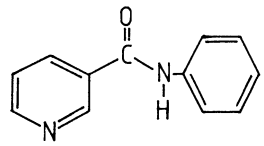

(IV) (nicotinoylanilide)

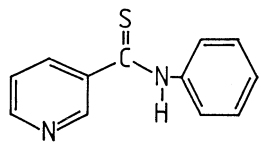

(V) (thionicotinoylanilide)

Experimental

Quinhydrone ($C_6H_6O_2^*$ $C_6H_4O_2$) (Merck), indigo ($C_{16}H_{10}N_2O_2$) (Sigma), acridine ($C_{13}H_9N$) (Merck), famotidine ($C_8H_{15}N_7O_2S_3$), probucol ($C_{13}H_{48}O_2S_2$), 6-propyl-2-thiouracil ($C_7H_{10}N_2OS$) (all Alkaloid, Skopje), HCl, H_2SO_4, KNO_3 and NaOH (all Merck, analytical grade) were used as received. Nicotinoylanilide ($C_{12}H_{10}N_2O$) and thionicotinoylanilide ($C_{12}H_{10}N_2S$) were synthesised at the University of Skopje [67, 68]. Water was doubly distilled. The solutions were buffered by 0.1 M buffer solutions pH 3.5 and 4.65 (sodium citrate-HCl), pH 5.5 (sodium citrate-NaOH), pH 6.5 and 8 (borax-KH_2PO_4), pH 9 (H_3BO_3-NaOH) and pH 11 (glycine-NaOH) (all chemical from Merck and Sigma, analytical grade).

Supporting electrolytes were 1 M HCl, 0.1 M H_2SO_4, 1 M KNO_3+10^{-2} M HCl, 1 M KNO_3, 0.1 M NaOH and 1 M KNO_3 buffered to various pH.

The working electrode was a spectral-grade paraffin-impregnated graphite rod (diameter 5 mm, length 50 mm). Its clean and carefully polished circular surface was contaminated with traces of solid organic compounds by pressing it into a small pile of substance powder on a highly glazed ceramic tile and moving it with a circular motion for about 10 s. A platinum gauze was an

auxiliary electrode, and Ag|AgCl|3 M KCl (Metrohm) was the reference electrode (E = 0.208 V vs SHE).

Cyclic staircase and square-wave voltammetric measurements were performed using a multimode polarograph (Autolab, EcoChemie, Utrecht), a personal computer and a printer.

Liquid electrolytes were degassed with high purity nitrogen for 20 min prior to the measurement. A nitrogen blanket was maintained thereafter. The cell was kept at 20 °C in a thermostat.

Results and Discussion

Quinhydrone

Cyclic voltammograms of quinhydrone microparticles are shown in Fig. 1. A pair of peaks I and II, at 0.73 V and −0.07 V, respectively, can be attributed to the oxidation of quinhydrone and the re-reduction of quinone:

$$Q{*}H_2Q \rightleftharpoons 2Q + 2e^- + 2H^+$$

A median potential of this redox reaction is $E_1 =$ 0.33 V, and the peak separation is 0.8 V. The cathodic and anodic peaks III and IV appear in the first cycle at the potentials −0.40 V and −0.05 V, respectively. They are attributed to the reduction of quinhydrone and the reoxidation of hydroquinone:

$$Q{*}H_2Q + 2e^- + 2H^+ \rightleftharpoons 2H_2Q$$

In the second and the fifth cycles the peak III appears at −0.31 V and −0.24 V, respectively. So, the median potential E_2 of this redox reaction changes from −0.175 V in the first cycle to −0.095 V in the fifth cycle and the peak separation decreases from 0.35 V to 0.19 V. The voltammetry of solid quinhydrone can be explained by the redox reaction $H_2Q \rightleftharpoons Q + 2e^- + 2H^+$ which is complicated by the stabilisation of intermediate $Q{*}H_2Q$. The theory of this type of reactions can be found in the literature [69], and here the difference between the median potentials E_1 and E_2 is briefly discussed. It is assumed that on the surface of the quinhydrone particle the hydrogen bonds between hydroquinone and quinone molecules can be broken under the influence of water molecules: $Q{*}H_2Q \rightleftharpoons Q + H_2Q$. So, a dissociation constant is defined: $K_0 = [Q][H_2Q]/[Q{*}H_2Q]$. It is also assumed that because of low solubility the molecules Q and H_2Q upon dissociation remain bound to the particle surface by charge transfer forces. Using the Nernst equation for the quinone-hydroquinone system $E = E_f + (RT/2F)\ \ln([Q]/[H_2Q])$ and the concentration of free hydroquinone molecules on the particle surface $[H_2Q] = K_0[Q{*}H_2Q]/[Q]$, the oxidation of quinhydrone is described by the equation: $E = E_f - (RT/2F)\ln K_0 + (RT/2F)\ln([Q]^2/[Q{*}H_2Q])$. For the reduction of quinhydrone the Nernst equation is: $E = E_f + (RT/2F)\ln K_0 + (RT/2F)\ln([Q{*}H_2Q]/[H_2Q]^2)$. Since $K_0 < 1$, the median potential E_1 is higher than E_f and the potential E_2 is smaller than E_f. Also, $E_f = (E_1 + E_2)/2$. It has been shown previously that under potentiometric conditions the formal potential of solid quinhydrone in a graphite powder composite electrode is $E_f = 0.692–0.058$ pH V vs SHE [70]. So, at pH 2 the formal potential is $E_f = 0.37$ V vs Ag | AgCl | 3 M KCl. In cyclic voltammetry the redox reaction of quinhydrone particles occurs at $(E_1+E_2)/2 = 0.12$ V, which is 0.25 V negative to the potentiometric value. This difference can not be explained by a simple theory presented here, probably because the reaction is kinetically controlled. Besides, the response diminishes during the repetitive cycling which indicates that particles are gradually dissolved.

The surface of the particles is in contact with the liquid electrolyte. The redox reaction of quinhydrone

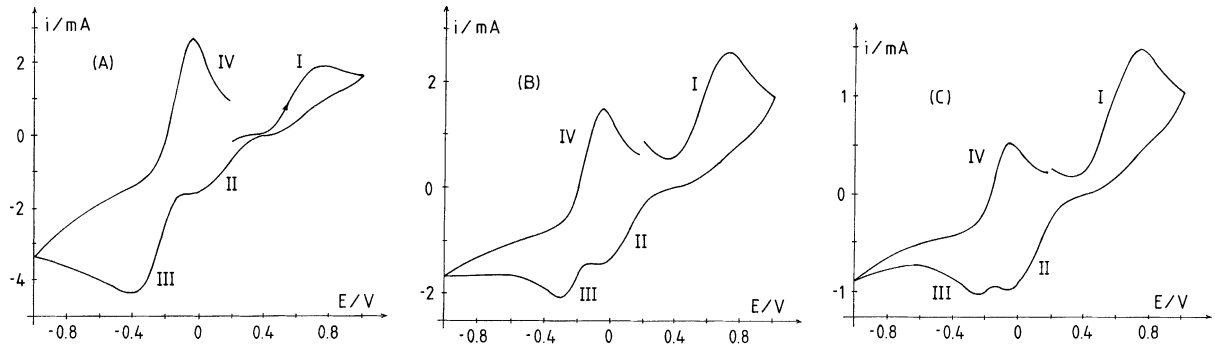

Fig. 1. Cyclic voltammetry of quinhydrone microparticles in 1 M KNO_3+10^{-2} M HCl. First (A), second (B) and fifth scan (C). Starting potential is 0.2 V, and scan rate is 0.1 V/s. The solid particles are mechanically transferred to the surface of the paraffin impregnated graphite electrode and immersed into a liquid electrolyte

requires water as the proton donor and proton acceptor. So, the rate of its propagation is the highest on the particle surface. Under chronoamperometric conditions, the current on the surface was calculated in the previous communication [45]:

$$I_S = nFb\Gamma(D_e/\pi t)^{1/2}(1+\exp(\varphi))^{-1}$$

where b is the length of the three-phase boundary and Γ is the formal surface concentration of quinhydrone. The current on the particle surface decreases with the square-root of time and depends solely on the surface diffusion coefficient D_e. So, the voltammetric response may appear even if protons can not diffuse through the microcrystal. The solution for cyclic voltammetry was discussed previously [41].

Indigo

A cyclic voltammogram of indigo microparticles in 0.1 M H_2SO_4 is shown in Fig. 2. It is characterized by two well developed pairs of peaks in full agreement with the results of Bond et al. [40]. The formal potentials ($E_f = (E_{P,a}+E_{P,c})/2$) of the redox systems I and II are linear functions of pH of the solutions with the slopes of −58 mV and −50 mV, respectively, as can be seen in Fig. 3. The two systems are not mutually dependent. By cycling between 0 and −0.6 V and between 0 and 0.7 V two steady-state responses are obtained. They are shown in Fig. 4. These results demonstrate that both reduction and oxidation of indigo microparticles are chemically reversible processes. Besides, the separations between the anodic and the cathodic peaks in Fig. 2 are 28 mV for the system I and 32 mV for the system II. This indicates that two electrons are exchanged in each redox

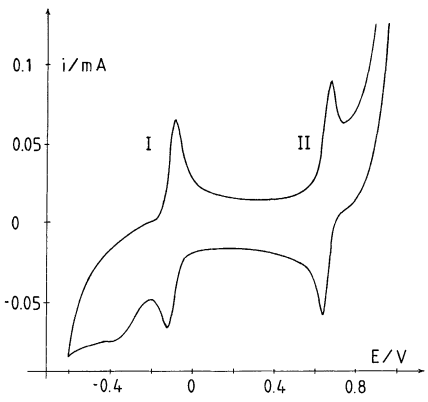

Fig. 2. Cyclic voltammetry of indigo microparticles in 0.1 M H_2SO_4. Second cyclic. Scan rate 1 V/s

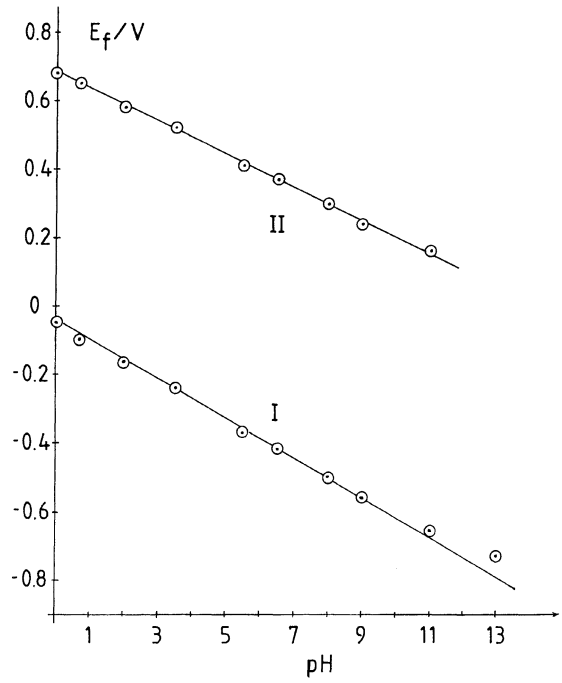

Fig. 3. Dependence of formal potentials of indigo redox systems I and II on pH of the solution. Scan rate 0.1 V/s

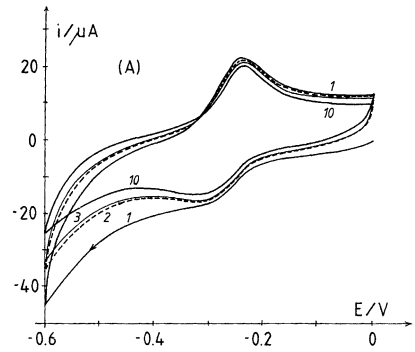

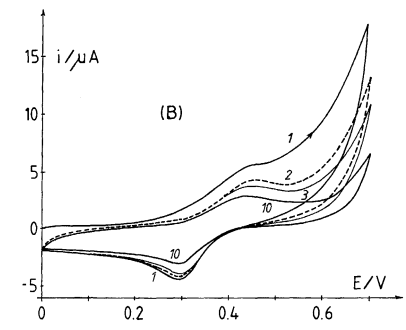

Fig. 4. Cyclic voltammetry of indigo microparticles in 1 M KNO_3 buffered to pH 3.5 (A) and 6.5 (B). Scan rates 1 V/s (A) and 0.1 V/s (B). The numbers of cycles are marked

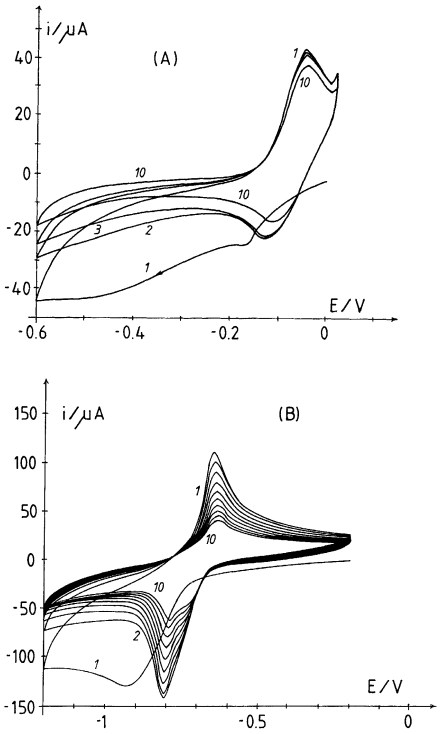

Fig. 5. Cyclic voltammetry of indigo microparticles in 1 M HCl (A) and 0.1 M NaOH (B). Scan rate 0.1 V/s

process. So, the redox system I can be attributed to the reduction of indigo to leucoindigo and its reoxidation, while the system II most probably corresponds to the oxidation of indigo to dehydroindigo and its subsequent re-reduction to indigo. Fig. 5 shows that the solubility of leucoindigo in the acidic solution is not significant, but in 0.1 M NaOH solution the peak currents continuously decrease because leucoindigo is partly dissolved. These experiments confirm the mechanism proposed by Bond et al. [40]. In unbuffered 1 M KNO_3 solution the formal potential of the indigo-leucoindigo redox reaction is more cathodic and the one of the indigo-dehydroindigo reaction is more anodic than in the buffered electrolyte. These shifts correspond to the local changes of pH at the surface of particles to pH 10 and pH 4, respectively, as a consequence of the consumption and the release of protons in these redox reactions. Regarding the assumed activation of the surface in the initial phase of redox reactions, we did not notice significant differences in peak potentials between the first and the subsequent cycles in neutral and moderate acidic media (see Fig. 4). However, in strongly acidic electrolytes (Figs. 2 and 5 A) a totally irreversible peak appears between −0.35 V and −0.45 V which partly masks the peak of the reduction of indigo. The origin of this peak is not known, but it disappears with the increasing of pH (see Fig. 4). In 0.1 M NaOH the potential of the indigo reduction in the first cycle is more negative than in the other cycles (see Fig. 5 B). This can be explained by the dissociation and dissolution of leucoindigo. In the first cycle neutral molecules of leucoindigo are formed by the reaction which includes two electrons and two protons. At first, these molecules are bound to the surface of particles, but gradually they dissociate to leucoindigo anions which are hydrated and then dissolved. The reoxidation of the anion includes two electrons, but one proton. By this initial cycle the surface is activated in the sense that it is covered by loosely bound indigo molecules which can be reduced and reoxidized in the redox reaction which includes two electrons and one proton. In the acidic and neutral electrolytes the faradaic peak is smaller in the first cycle than in the other cycles because the capacitive component of the response appears the biggest in the first cycle, but the potentials of all peaks are similar, except in 1 M HCl. So, the proposed "break in" process is not necessarily the initial phase of the redox mechanism at all pH values.

The peak separation which is shown in Fig. 2 is not characteristic for all electrolytes. The average difference between the cathodic and anodic peaks change from 50 mV in the acidic media to 150 mV in basic media. This is caused by different slopes of linear relationship between cathodic and anodic peak potentials and pH of solutions. In the redox system I the slopes are −63 mV and −54 mV for the cathodic and anodic peaks, respectively. In the second system the slopes are −45 mV and −55 mV for the anodic and cathodic reactions, respectively. However, in 1 M KNO_3+10^{-2} M HCl the peak potentials of the system I do not change if the scan rate is increased from 5 mV/s to 1 V/s, which suggests that this redox reaction is fast and reversible. So, the peak separation can be explained only by the incomplete proton exchange. It seems that even in the buffered electrolytes the redox reactions may cause the local changes of pH near the surface of particles.

The relationship between the peak currents of the redox system I at pH 2 and the scan rate is: $I_p = k \cdot v^{0.7}$. Similar dependence was observed in the voltammetry of azobenzene microparticles [41]. It was explained by the diffusion in the restricted space. Starting from the three-phase boundary the electrons

are propagated over the surface of particles by a diffusion-like process. So, the current depends on the size of particles. If the size is very small, the current is directly proportional to the scan rate as in the surface reaction, but if the particle is rather large the current is proportional to the square-root of the scan rate. Thus, the observed relationship between the peak currents and the scan rate is an average response of many particles with different sizes.

Square-wave voltammetry is a very useful technique for the fast inspection of electroactive solids [32]. The response of indigo microparticles immersed in the acidic electrolyte is shown in Fig. 6A. The starting potential is 1 V and the frequency is 100 Hz. The potentials of peaks I and II are very close to the formal potentials of the systems I and II in Fig. 3. The cathodic and anodic components of the square-wave response, which are shown in Fig. 6B, indicate that the redox reactions I and II are fast and reversible. These components also show that the third peak appearing at −0.36 V is the response of a totally irreversible reaction. The potentials of peaks I and II depend linearly on pH of electrolytes with the slope of −55 mV and −60 mV, respectively. The variation of frequency between 10 Hz and 1000 Hz has no influence on these peak potentials, which is all in agreement with the results of cycling voltammetry. Fig. 7 shows that in 0.1 M NaOH the square-wave response of the system I is significantly enhanced. This can be explained by the mobility of partially dissolved leucoindigo anions. The cathodic component of the response, which corresponds to the re-reduction of indigo, is an indication of a quasi-reversible charge transfer [17].

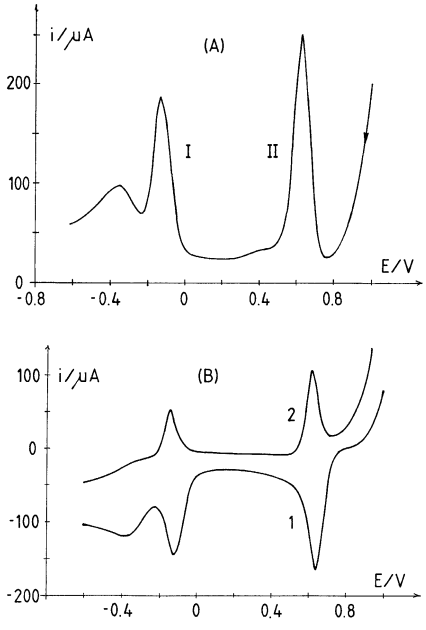

Fig. 6. Square-wave voltammetry of indigo microparticles in 1 M KNO_3+10^{-2} M HCl. Nett response (A) and its forward *(1)* and backward *(2)* components (B). Starting potential 1 V, frequency 100 Hz, amplitude 50 mV and potential increment 5 mV

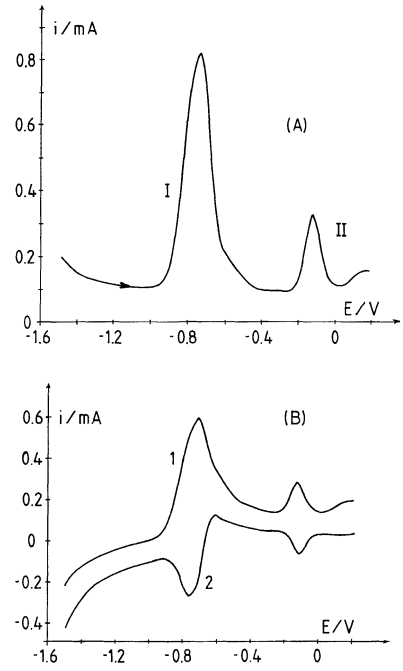

Fig. 7. Square-wave voltammetry of indigo microparticles in 0.1 M NaOH. Nett response (A) and its forward *(1)* and backward *(2)* components (B). Starting potential −1.5 V. All other data as in Fig. 6

Acridine

Cyclic voltammograms of acridine microparticles are shown in Fig. 8. The response is characterised by the cathodic peaks I and II at −0.5 V and −1.2 V, respec-

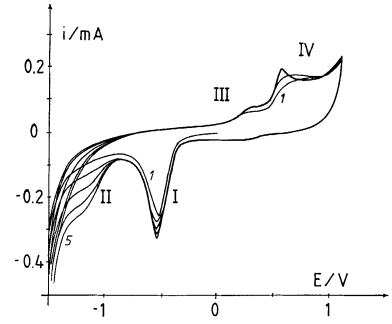

Fig. 8. Cyclic voltammetry of acridine microparticles in 1 M KNO_3+10^{-2} M HCl. Scan rate 0.1 V/s

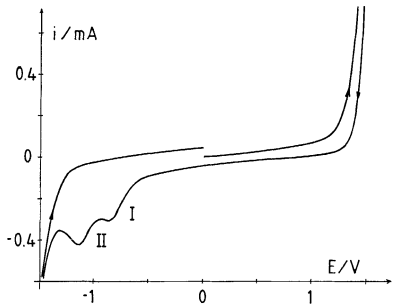

Fig. 9. Cyclic voltammogram of acridine microparticles in 1 M KNO_3 buffered to pH 9. The first cycle is shown. Initial scan direction is from 0 V to 1.5 V. Scan rate is 0.1 V/s

tively, and the anodic peaks III and IV at 0.3 V and 0.6 V, respectively. The starting potential is 0 V and the initial scan direction is towards −1.5 V. If the cycling starts from 0 V to 1.5 V, the anodic peaks III and IV do not appear in the first cycle as can be seen in Fig. 9, but they appear in the second and the subsequent cycles. These peaks also appear if the potential is reversed at −1 V. At pH 9, the first cathodic peak appears at −0.8 V, but the potentials of the peaks II, III and IV are independent of pH of the electrolyte. These results indicate that the peaks I, III and IV correspond to the electroreduction of acridine and the reoxidation of the product:

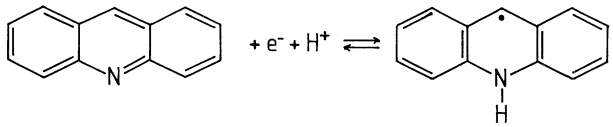

This redox reaction is electrochemically irreversible, as can be concluded from the very large separation of the cathodic and anodic peaks. For this reason the peaks III and IV do not depend on pH, while the peak I is pH dependent. The second cathodic peak is the consequence of a totally irreversible reduction of monohydroacridine radical to dihydroacridine:

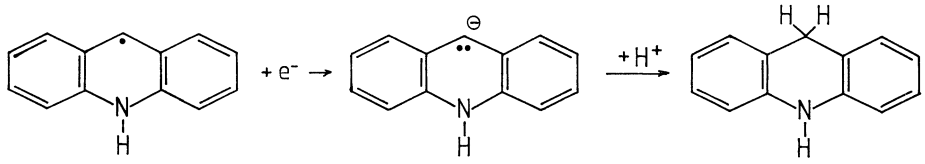

At pH 2, acridine is partly protonated on the surface of particles and the first redox reaction is:

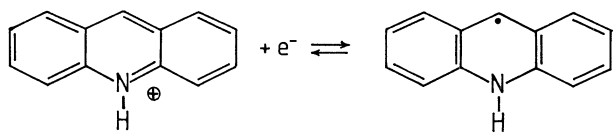

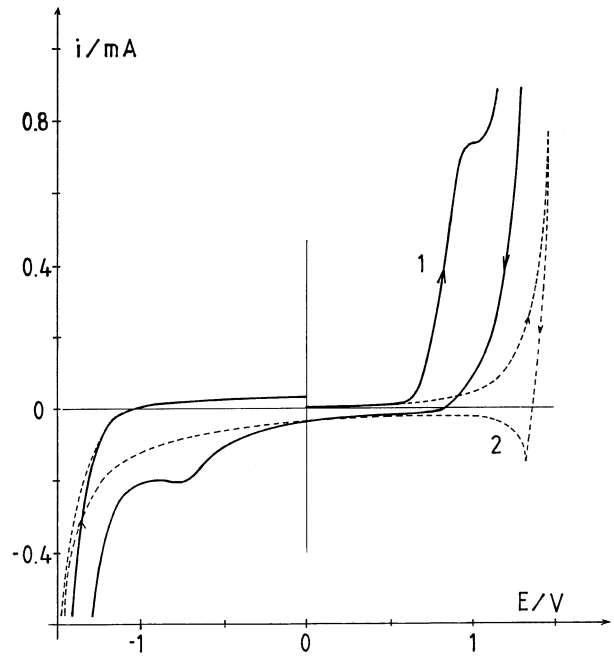

Fig. 10. Cyclic voltammetry of famotidine microparticles in 1 M KNO_3 buffered to pH 4.65. The first cycle is shown *(1)*. Starting potential 0 V and scan rate 0.1 V/s. The curve *(2)* is the response of bare electrode

This simple mechanism does not explain why there are two anodic peaks III and IV but there is not enough experimental evidences to speculate about different forms of the monohydroacridine radical on the particle surface. Besides, the protonation in the acid medium increases the solubility of acridine in water. Hence, the enhancement of peak currents observed during the repetitive cycling is probably caused by the mobility of acridine molecules.

Famotidine

Fig. 10 shows the cyclic voltammogram of famotidine microparticles. It is marked by the anodic peak at 1 V and the cathodic peak at −0.8 V. Both peaks are diminished by the repetitive cycling and eventually vanish. The potential window of bare electrode is shown by curve 2 in Fig. 10. As the anodic process starts at about 0.7 V, the cathodic peak appears at −0.7 V if the potential is cycled between 0.9 V and −0.9 V. However, if the initial scan direction is from

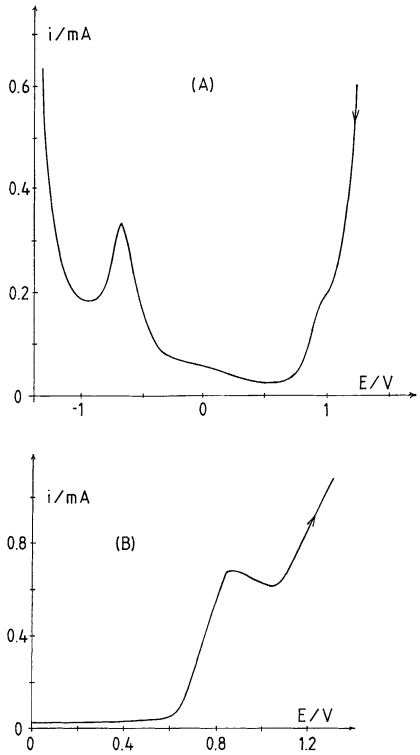

Fig. 11. Square-wave voltammetry of famotidine. Starting potentials 1.3 V (A) and 0 V (B) and scan directions are marked by arrows. Frequency 100 Hz, amplitude 50 mV and a step increment 5 mV. All other data as in Fig. 10

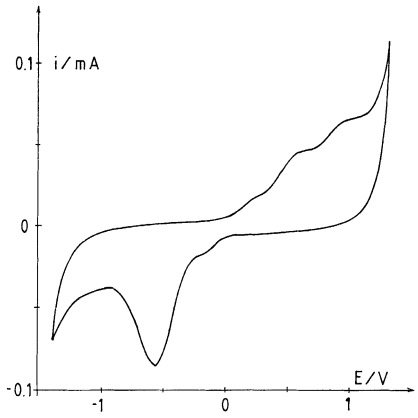

Fig. 12. Cyclic voltammetry of probucol microparticles in 1 M KNO_3 buffered to pH 4.65. Scan rate is 0.1 V/s

0 V to −1.5 V, the cathodic peak does not appear in the first cycle. In square-wave voltammetry the peak corresponding to a totally irreversible reduction appears at −0.675 V if the starting potential is higher than 0.9 V (Fig. 11 A). If the starting potential is lower than 0.4 V, the peak corresponding to a totally irreversible oxidation appears at 0.84 V (Fig. 11B). The peak at −0.7 V does not appear even if the starting potential is as negative as −1.5 V. These results indicate that famotidine is oxidized at 0.84 V and that the product of this oxidation is reduced at −0.675 V, but not back to famotidine. These two redox reactions can not establish a steady state and the response vanishes. At this point it is not possible to locate the electroactive centers in the famotidine molecule.

Probucol

A redox reaction of solid probucol attains a steady state in cyclic voltammetry (Fig. 12). Two oxidation peaks appear at 0.55 V and 0.98 V and the reduction

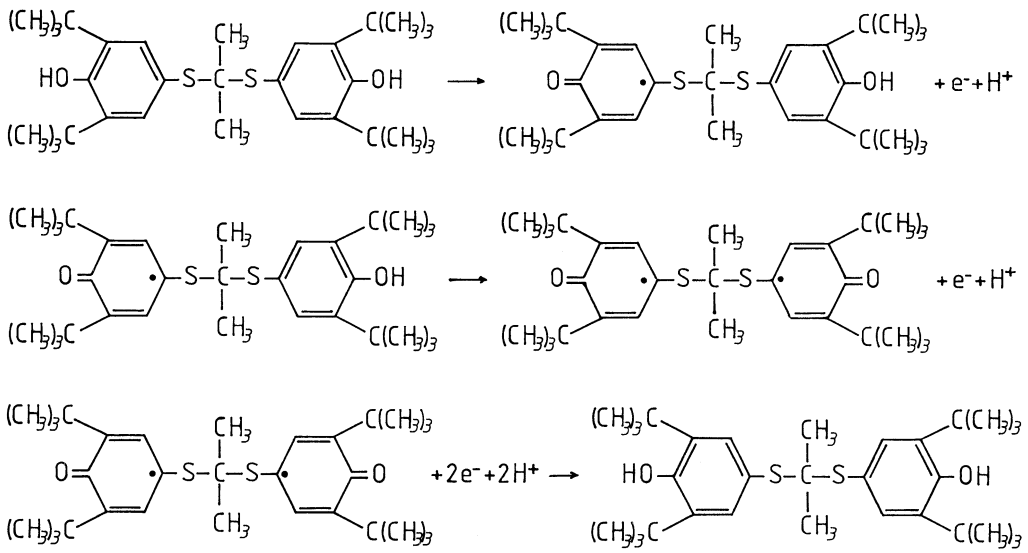

Scheme 3

peak appears at −0.54 V. The reduction peak does not appear in the first cycle if the initial scan direction is from 0 V to −1.3 V. This response can be attributed to a stepwise oxidation of probucol to a semiquinone radical and a disemiquinone radical which is reduced back to probucol in the electrochemically irreversible process (Scheme 3).

Additional investigations to verify the assumed redox mechanism are currently in progress [71].

Propylthiouracil

A cyclic voltammogram of propylthiouracil microparticles is characterised by the oxidation at 0.73 V and the reduction at −0.77 V (Fig. 13). Square-wave voltammetry indicates that both processes are electrochemically irreversible, but together they maintain a steady state in cyclic voltammetry. The reduction peak appears only if it is preceded by the oxidation, so it corresponds to re-reduction of the oxidation product back to propylthiouracil.

Thionicotinoylanilide

A linear scan voltammogram of solid thionicotinoylanilide is shown in Fig. 14. A peak corresponding to a totally irreversible reduction appears at −0.36 V. In cyclic voltammetry no oxidation peak was observed within the available potential window. The reduction peak vanishes after few cycles. Similar response was obtained in linear scan voltammetry of solid nicotinoylanilide, but the peak current was ten times smaller.

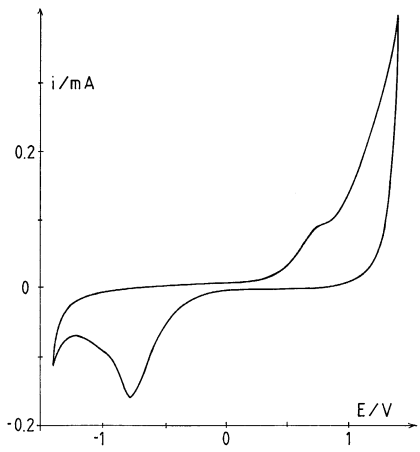

Fig. 13. Cyclic voltammetry of propylthiouracil microparticles in 1 M KNO_3 buffered to pH 4.65. Scan rate is 0.1 V/s

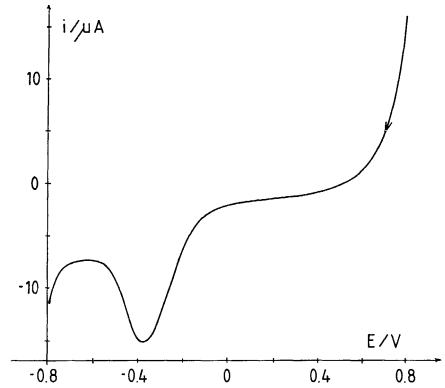

Fig. 14. Linear scan voltammetry of thionicotinoylanilide microparticles in 1 M KNO_3 buffered to pH 4. Starting potential 0.8 V and a scan rate 0.1 V/s

The described results show that electrochemical properties of some organic compounds can be measured without dissolving the sample. This can be useful for a direct identification of powder substances. As only a minute amount of sample is needed, a qualitative microanalytical methods for pharmacology can be developed.

References

[1] F. Scholz, B. Meyer, In: A. J. Bard, I. Rubinstein (eds.) *Electroanal. Chem.* Vol. 20 Dekker, New York, 1998, p. 1.
[2] V. I. Belyi, T. P. Smirnova, N. F. Zakharchuk, *Appl. Surf. Sc.* **1989**, *39*, 161.
[3] S. Zhang, B. Meyer, G. Moh, F. Scholz, *Electroanalysis*, **1995**, *7*, 319.
[4] F. Scholz, W. D. Müller, L. Nitschke, F. Rabi, L. Livanova, C. Fleischfresser, C. Thierfelder, *Fresinius J. Anal. Chem.* **1990**, *338*, 37.
[5] F. Scholz, A. Dostal, *Angew. Chem.* **1995**, *107*, 2876.
[6] Š. Komorsky-Lovrić, J. Bartoll, R. Stösser, F. Scholz, *Croat. Chem. Acta* **1997**, *70*, 563.
[7] Š. Komorsky-Lovrić, *Croat. Chem. Acta* **1998**, *71*, 263.
[8] Š. Komorsky-Lovrić, *Electroanalysis*, **1999**, *11*, 120.
[9] F. Scholz, B. Lange, *Trends. Anal. Chem.* **1992**, *11*, 359.
[10] F. Scholz, B. Meyer, *Chem. Soc. Rev.* **1994**, *23*, 341.
[11] F. Scholz, L. Nitschke, G. Henrion, F. Damaschun, *Fresenius Z. Anal. Chem.* **1989**, *335*, 189.
[12] B. Lange, F. Scholz, H. J. Bautsch, F. Damaschun, G. Wappler, *Phys. Chem. Minerals* **1993**, *19*, 489.
[13] B. Meyer, B. Ziemer, F. Scholz, *J. Electroanal. Chem.* **1995**, *392*, 79.
[14] T. Grygar, J. Šubrt, J. Bohaček, *Collect. Czech. Chem. Commun.* **1995**, *60*, 950.
[15] T. Grygar, *J. Electroanal. Chem.* **1996**, *405*, 117.
[16] T. Grygar, *J. Solid State Electrochem.* **1997**, *1*, 77.
[17] Š. Komorsky-Lovrić, M. Lovrić, A. M. Bond, *Anal. Chim. Acta* **1992**, *258*, 299.
[18] F. Scholz, L. Nitschke, G. Henrion, *Electroanalysis* **1990**, *2*, 85.
[19] F. Scholz, F. Rabi. W. D. Müller, *Electroanalysis* **1992**, *4*, 339.

[20] R. E. Dueber, A. M. Bond, P. G. Dickens, *J. Electrochem. Soc.* **1992**, *139*, 2363.
[21] U. Schröder, F. Scholz, *J. Solid State Electrochem.* **1997**, *1*, 62.
[22] A. M. Bond, J. B. Cooper, F. Marken, D. M. Way, *J. Electroanal. Chem.* **1995**, *396*, 407.
[23] A. Dostal, U. Schröder, F. Scholz, *Inorg. Chem.* **1995**, *34*, 1711.
[24] A. Dostal, B. Meyer, F. Scholz, U. Schröder, A. M. Bond, F. Marken, S. J. Shaw, *J. Phys. Chem.* **1995**, *99*, 2096.
[25] N. F. Zakharchuk, B. Meyer, H. Henning, F. Scholz, A. Jaworski, Z. Stojek, *J. Electroanal. Chem.* **1995**, *398*, 23.
[26] S. J. Reddy, A. Dostal, F. Scholz, *J. Electroanal. Chem.* **1996**, *403*, 209.
[27] A. Dostal, G. Kauschka, S. J. Reddy, F. Scholz, *J. Electroanal. Chem.* **1996**, *406*, 155.
[28] A. Dostal, M. Hermes, F. Scholz, *J. Electroanal. Chem.* **1996**, *415*, 133.
[29] A. M. Bond, F. Scholz, *J. Phys. Chem.* **1991**, *95*, 7460.
[30] A. M. Bond, R. Colton, F. Daniels, D. R. Fernando, F. Marken, Y. Nagaosa, R. F. M. Van Steveninck, J. N. Walter, *J. Am. Chem. Soc.* **1993**, *115*, 9556.
[31] A. M. Bond, R. Colton, F. Marken, J. N. Walter, *Organometallics* **1994**, *13*, 5122.
[32] Š. Komorsky-Lovrić, *J. Electroanal. Chem.* **1995**, *397*, 211.
[33] A. J. Downard, A. M. Bond, L. R. Hanton, G. A. Heath, *Inorg. Chem.* **1995**, *34*, 6387.
[34] S. J. Show, F. Marken, A. M. Bond, *J. Electroanal. Chem.* **1996**, *404*, 227.
[35] Š. Komorsky-Lovrić, M. Lovrić, F. Scholz, *Mikrochim. Acta* **1997**, *127*, 95.
[36] A. M. Bond, R. Colton, P. J. Mahon, W. T. Tan, *J. Solid State Electrochem.* **1997**, *1*, 53.
[37] A. M. Bond, S. Fletcher, F. Marken, S. J. Shaw, P. G. Symons, *J. Chem. Soc. Faraday Trans.* **1996**, *92*, 3925.
[38] S. J. Shaw, F. Marken, A. M. Bond, *Electroanalysis* **1996**, *8*, 732.
[39] S. J. Reddy, M. Hermes, F. Scholz, *Electroanalysis* **1996**, *8*, 955.
[40] A. M. Bond, F. Marken, E. Hill, R. G. Compton, H. Hügel, *J. Chem. Soc. Perkin Trans.* **1997**, *2*, 1735.
[41] Š. Komorsky-Lovrić, *J. Solid State Electrochem.* **1997**, *1*, 94.
[42] L. Roullier, E. Waldner, E. Laviron, *J. Electrochem. Soc.* **1985**, *132*, 1121.
[43] A. Jaworski, Z. Stojek, F. Scholz, *J. Electroanal. Chem.* **1993**, *354*, 1.
[44] A. M. Bond, F. Marken, *J. Electroanal. Chem.* **1994**, *372*, 125.
[45] M. Lovrić, F. Scholz, *J. Solid State Electrochem.* **1997**, *1*, 108.
[46] A. I. Vogel, *Practical Organic Chemistry*, Longmans, London, 1959, p. 747.
[47] T. Sakurai, *Acta Cryst. B* **1968**, *24*, 403.
[48] C. K. Mann, K. K. Barnes, *Electrochem. React. Nonaqueous Syst*. Dekker, New York, 1970, p. 190.
[49] Y. B. Shim, S. M. Park, *J. Electroanal. Chem.* **1997**, *425*, 201.
[50] J. H. Baxendale, H. R. Hardy, *Trans. Faraday Soc* **1953**, *49*, 1140.
[51] Š. Komorsky-Lovrić, M. Lovrić, *Croat. Chem. Acta* **1991**, *64*, 625.
[52] R. Luckenbach (ed.) *Beilsteins Handbuch der Organischen Chemie, Vol. 24*. Springer, Berlin Heidelberg New York, 1981, p. 1791.
[53] T. Bechtold, E. Burtscher, A. Turcanu, O. Bobleter, *J. Electrochem. Soc.* **1996**, *143*, 2411.
[54] D. A. Hall, P. J. Elving, *Israel J. Chem.* **1970**, *8*, 839.
[55] Y. Li, S. Dong, *J. Electroanal. Chem.* **1993**, *348*, 181.
[56] K. Ogura, I. Yoshida, *Electrochim. Acta* **1987**, *32*, 1191.
[57] D. Grosjean, P. M. Whitmore, G. R. Cass, J. R. Druzik, *Environ. Sci. Technol.* **1988**, *22*, 292.
[58] G. Beggiato, G. Casalbore-Miceli, A. Geri, D. Pietropaolo, *Ann. Chim.* **1993**, *83*, 355.
[59] K. Uehara, K. Takagishi, M. Tanaka, *Solar Cells* **1987**, *22*, 295.
[60] R. C. Kaye, H. I. Stonehill, *J. Chem. Soc.* **1951**, 27.
[61] V. Zanker, H. Schnith, *Chem. Ber.* **1959**, *92*, 2210.
[62] H. Baumgärtel, K. J. Retzlav, in A. J. Bard, H. Lund (eds.) *Encyclopedia of Electrochemistry of the Elements, Vol. XV.* Dekker, New York, 1984, p. 226.
[63] S. Budavari (ed.) *The Merck Index.* Merck, Rahway, N. J., 1989, pp. 617, 1230, 1475.
[64] J. A. Squella, C. Rivera, I. Lemus L. J. Nunez-Vergara, *Mikrochim. Acta.* **1990**, *I*, 343.
[65] V. Mirčeski, B. Jordanoski, Š. Komorsky-Lovrić, *Portugaliae Electrochim. Acta* **1998**, *16*, 43.
[66] J. Q. Chambers, in A. J. Bard, H. Lund (eds.) *Encyclopedia of Electrochemistry of Elements, Vol. XII*, Dekker, New York, 1978, p. 329.
[67] M. B. Robin, F. A. Bovey, M. Basch, *The Chemistry of Amides.* In: J. Zabicky (ed.) Interscience, London, 1970, p. 1.
[68] W. Walter, J. Vos, *The Chemistry of Thioamides*, In: J. Zabicky (ed.) Wiley, New York, 1970, p. 327.
[69] M. Lovrić, *J. Electroanal. Chem.* **1983**, *153*, 1.
[70] H. Düssel, Š. Komorsky-Lovrić, F. Scholz, *Electroanalysis* **1995**, *7*, 889.
[71] V. Mirćeski, M. Lovrič, B. Jordanoski, *Electroanalysis* 1999, 11 (in press).

Received September 22, 1998. Revision March 19, 1999.